

Supporting information for

Color variation in radio-luminescence of P-dots doped with thermally activated delayed fluorescence molecules.

Zheming Su,^{a,#} Hieu Thi Minh Nguyen,^{b,#} Zuoyue Liu,^a Daiki Asanuma,^a Minoru Yamaji,^c Masanori Koshimizu,^d Hajime Shigemitsu,^e Sachiko Tojo,^a Tadashi Mori,^e Toshiyuki Kida,^e Guillem Pratx,^{b*} Mamoru Fujitsuka,^{a,f*} and Yasuko Osakada^{a,f*}

a. SANKEN (The Institute of Scientific and Industrial Research), Osaka University, Mihogaoka 8-1, Ibaraki, Osaka 567-0047 (Japan).

b. Department of Radiation Oncology and Medical Physics, Stanford University, 3172 Porter Dr, Palo Alto, CA 94304 (USA).

c. Division of Molecular Science, Graduate School of Science and Engineering, Gunma University, Ota, Gunma 373-0057 (Japan).

d. Research Institute of Electronics, Shizuoka University, 3-5-1 Johoku, Naka-ku, Hamamatsu, 432-8011 (Japan).

e. Department of Applied Chemistry, Graduate School of Engineering, Osaka University, 2-1 Yamadaoka, Suita, Osaka 565-0871, (Japan).

f. Innovative Catalysis Science Division, Institute for Open and Transdisciplinary Research Initiatives (ICS-OTRI), Osaka University, 2-1 Yamadaoka, Suita, Osaka 565-0871, (Japan).

These authors contributed equally to this work.

Materials and methods.

10,10'-(4,4'-Sulfonylbis(4,1-phenylene))bis(9,9-dimethyl-9,10-dihydroacridine) (DMAC-DPS, **1**) 1,2,3,5-Tetrakis(carbazol-9-yl)-4,6-dicyanobenzene,2,4,5,6-Tetrakis(9H-carbazol-9-yl) isophthalonitrile (4CzIPN, **2**), and polyvinylcarbazole (PVK) were purchased from Sigma-Aldrich (St. Louis, Missouri, United States). 10,10'-(11,12-Di-o-tolyldibenzo[a,c]phenazine-3,6-diyl)bis(10H-phenoxazine) (oDTBPZ-DPXZ, **3**) was purchased from luminescence technology corp (New Taipei City, Taiwan). PEG polymer was purchased from polymer source (Quebec, Canada). Tetrahydrofuran (THF) was purchased from FUJIFILM Wako (Osaka, Japan). Poly(vinyl alcohol) (PVA) was purchased from TCI (Tokyo, Japan). All chemicals were used as received without any further purification.

Synthesis of P-dots.

Thermally activated delayed fluorescence (TADF) molecules doped P-dots were synthesized according to our previous report.¹ Stock solutions of PVK, PEG-COOH polymers, and TADF molecules were prepared by dissolving each component in THF at a concentration of 1 mg/ml. Then, PVK solution 30 μ L, PEG-COOH solution 60 μ L, TADF solution 150 μ L and THF solution 60 μ L were mixed and sonicated for 5 minutes to achieve a homogenous mixture. For doping concentration dependent

photoluminescence experiment, we added the amount of TADF solution in the Table S4. The resulting solution was then gradually dispersed into 1 mL of milliQ water at a rate of 20 μ L per increment under continuous sonication, followed by an additional 5 minutes of sonication. THF was then removed by centrifugal evaporation and water was added to synthesize a total of 1 mL of aqueous P-dots solution.

Fabrication of P-dots film.

Films were obtained by mixing the polymer matrix and concentrated P-dots solution in a 1:1 ratio, followed by water evaporation. For the polymer matrix, 2.0 g PVA ($n = 1700$) was dissolved in 20 ml milliQ water and stirred at 120 $^{\circ}$ C for 30 min. Subsequently, 1 mL PEG ($M_w = 200$) was added to the PVA solution, and the polymer matrix was finalized by continuous stirring at 90 $^{\circ}$ C for an additional 30 min. For concentrated P-dots solution, 10 mL of the P-dots solution was centrifuged in a 10 mL centrifugal tube at 3000 g and 15 $^{\circ}$ C for 8 minutes. After centrifugation, 0.5 mL (20-fold concentration) of concentrated P-dots solution was obtained. The concentrated P-dots solution and polymer matrix were added to a 1.5 ml tube at a 1:1 ratio and mixed. After dropping 0.2 mL of the mixed solution on the surface of the plastic petri dish, films were obtained by drying at 50 $^{\circ}$ C. Five films were then laminated together to form a thick film.

General characterization.

Emission spectra were measured at various temperature using a FP-8200 fluorescence spectrometer (JASCO, Tokyo, Japan) with slit size of 5 nm for excitation and emission channels equipped with temperature controlled unit. Absorption spectra were measured at room temperature using a V630 UV-visible spectrophotometer (JASCO, Tokyo, Japan). The hydrodynamic diameter of P-dots was measured by dynamic light scattering (DLS) using a Zetasizer Nano ZS (Malvern Panalytical, UK). The sample solution of P-dots were directly added into disposal cuvette and the averaged size was measured by three measurements. The morphology of P-dots particles was observed by transmission electron microscopy (TEM) measurements using an ultra-high resolution analytical electron microscope JEM-ARM200F (JEOL, Tokyo, Japan). For samples utilized in TEM measurements, synthesized P-dots solution was sonicated for 1 min, and subsequently, 10 μ L solution was dropped on the polymer coated Cu grid. The sample was obtained after complete drying. The analysis of particle size was conducted using ImageJ software by extracted 100 particles from the resulting TEM images. Quantum yields of photoluminescence were measured under aerobic and degassing conditions using a Quantaaurus-QY absolute PL quantum yield measurement system (HAMAMATSU Ptohonics K.K., Shizuoka, Japan) at an excitation wavelength of 355 nm. All degassing

procedures in the experiment were accomplished through 10 minutes of argon gas bubbling.

Photo-luminescence lifetime measurement.

Photo-luminescence lifetime was measured at room temperature using the photon counting method with a Quantaaurus-Tau compact fluorescence lifetime measurement system C11367 (HAMAMATSU Photonics K.K., Shizuoka, Japan) If it is stated, it was measured with a temperature controller. Measurements were conducted under both aerobic and degassing conditions. Curve fitting were performed by three-component exponential equation ($y = y_0 + A_1 * \exp(-x_1 / \tau_1) + A_2 * \exp(-x_2 / \tau_2) + A_3 * \exp(-x_3 / \tau_3)$), $\tau = \Sigma A_i \tau_i^2 / \Sigma A_i \tau_i$).

Laser flash photolysis experiment by Randomly-Interleaved-Pulse-Train (RIPT) method and nanosecond multichannel acquisition method.

Pico second transient absorption was measured at room temperature using the RIPT method with the picosecond transient absorption spectroscopy system picoTAS (UNISOKU, Osaka, Japan).² RIPT is a method where a pump pulse and a train of multiple probe pulses from a picosecond super continuum light source are not synchronized. For each pump pulse, numerous monochromatic probe pulses impinge upon the sample, and the associated pump-probe time delays are determined passively shot by shot with sub-

nanosecond accuracy. By repeatedly pumping with automatically varying time delays, transient absorption time profiles covering a wide dynamic range from sub-nanoseconds to milliseconds can ultimately be obtained simultaneously. Samples were adjusted to an absorbance of 1.0 at 355 nm, and measurements were performed under both aerobic (air) and degassed conditions (Ar). The experimental conditions were set as follows: pump frequency: 1000 Hz; accumulation number \times pump: 250 \times 500. Curve fitting performed by origin software using two-component exponential equation ($y = y_0 + A_1 * \exp(-x_1 / \tau_1) + A_2 * \exp(-x_2 / \tau_2)$, $\tau = \Sigma A_i \tau_i^2 / \Sigma A_i \tau_i$). Nanosecond multi-channel acquisition method was done by previously described by us.¹

Pulse radiolysis and electron beam excited photoluminescence measurements.

Nano-second transient absorption measurements via pulsed radiolysis method were conducted using a multichannel spectrometer with an L-band LINAC-accelerated electron pulse (28 MeV) as the excitation source. Measurements were carried out at room temperature under both aerobic and degassing conditions. Samples in toluene were diluted to achieve an absorbance of 1.0 at 355 nm. Measurements were carried out at room temperature under degassing conditions.

Hard-X-ray excitation experiments.

X-ray luminescence was produced by irradiating the samples using a small-animal

X-ray irradiator (PXI XRAD 320, North Branford, CT, USA). The X-ray beam (60 kVp and 40 mA, unfiltered) was directed toward the P-dots films positioned approximately 30 cm beneath the X-ray aperture. The luminescence emitted after radiation was directed to a CCD camera mounted perpendicular to the axis of the radiation beam through a mirror. We acquired the X-ray luminescence images with an exposure time of 30 seconds and a 4-pixel binning using the In-Vivo F Pro software. We utilized MATLAB (MathWorks, Natick, MA, USA) to filter radiation noise from the raw camera images and to display the luminescence intensity.

To examine the scintillation emission spectra of the P-dots samples, we excited these samples with an X-ray beam operated at 60 kVp and 40 mA using the PXI XRAD 320 X-ray irradiator. The X-ray beam was aimed directly at the film samples positioned immediately beneath the X-ray aperture to maximize the absorbed dose rate and light intensity. The film samples were placed atop the distal end of a 1 mm-core-diameter optical fiber (FP1000ERT, 0.5 NA, Thorlabs, Newton, NJ, USA), while the proximal end was coupled to the spectrometer. We measured the emission spectra using an optical spectrometer (Sensline, Avantes, Lafayette, CO, USA). Each film sample was measured three times with an exposure time of

5 seconds each for averaging. The spectral signals were then corrected by subtracting the background signal from a non-doped control film and adjusting for the non-uniform sensitivity of the spectrometer across various wavelengths. Finally, the spectra were normalized and smoothed using a Savitzky–Golay filter in MATLAB. We specifically chose a single pass with a third polynomial order and a small frame length of approximately 78 nm in spectrum length.

Single photon-counting for scintillation decay measurement.

The scintillation decay curves were obtained using a time-correlated single photon-counting method using multiple gamma rays as the excitation source, which is called a delayed coincidence method.³ ^{22}Na (~100 kBq) was used as the gamma-ray source, which emit almost simultaneously a 1.27-MeV gamma-ray photon and a positron. The positron annihilates with a nearby electron to produce two 511-keV gamma-ray photons within several hundred ns. Hence, three gamma-ray photons are generated within several hundred ns. A scintillation detector equipped with a plastic scintillator (Pilot-U, OKEN) was used to determine the timing of the gamma-ray generation. The ^{22}Na source was placed in front of the scintillation detector. The sample scintillators were placed on the opposite side of the source. The gamma-ray photons induce the scintillation from the samples, which was

detected using a photomultiplier tube (PMT; R7400P, Hamamatsu) placed at ~5 cm away from the sample to assure that less than one scintillation photon was detected by the PMT for scintillation event induced by a gamma-ray photon. The timing of the detection signals from the scintillation detector and the PMT were determined using a constant fraction discriminator (CFD; 935, Ortec). The timing signals originating from the scintillation detector and the PMT were used as the stop and start signals for a time-to-amplitude converter (TAC; 566 Ortec). Finally, the output signal of the TAC was supplied to a multichannel analyzer (MCA-8000D, Amptek) to obtain a histogram of the time difference between the production of gamma-ray photons and scintillation photons as the scintillation decay curve. The time resolution was approximately 1 ns.

P-dots stability test for gamma-ray irradiation.

Gamma ray radiation was used to measure the stability of P-dots. The gamma irradiation were conducted using the cobalt-60 gamma-ray irradiation system at Osaka University. The radiation source (Rabbit11) was irradiated at a dose rate of 17.45 Gy/h from a distance of 1 m for 30 or 60 min. After the irradiation experiments, the absorption spectra, photoluminescence spectra excited at 355 nm, and hydrodynamic diameter of the P-dots were measured.

Table S1. Photo-luminescent characteristics for TADF monomers.

Samples	λ_{\max}^a (nm) ^a	<i>FWHM</i> (nm)	Φ_{PL}^b (Ar) ^b	Φ_{PL}^b (Air) ^b	$\Phi_{\text{PL}}(\text{Air})/\Phi_{\text{PL}}(\text{Ar})$
1	465	76	0.50	0.12	0.24
2	510	74	0.73	0.23	0.32
3	600	72	0.22	0.09	0.41

^a Photoluminescence λ_{\max} . ^b Absolute quantum yields of photoluminescence.

Table S2. The averaged sizes of P-dots measured by TEM.

Sample	TEM (nm)
P-dots (1)	96
P-dots (2)	88
P-dots (3)	95

Table S3. The averaged sizes of P-dots measured by DLS before and after gamma-ray irradiation.

Sample	0 min (nm)	30 min (nm)	60 min (nm)
P-dots (1)	142	144	143
P-dots (2)	126	129	125
P-dots (3)	69	68	69

Table S4. Synthetic condition for individual P-dots at the volume of THF solution preparation.

(μL)*							
1, 2 or 3	0	30	60	90	120	150	180
PEG-COOH	60	60	60	60	60	60	60
PVK	30	30	30	30	30	30	30
THF	210	180	150	120	90	60	30

*Stock solutions of PVK, PEG-COOH polymers, and TADF molecules were prepared by dissolving each component in THF at a concentration of 1 mg/ml. The above materials were mixed in the above volume ratio and adjusted as a THF solvent. These were dispersed in 1 mL of water to make P-dots for a doping concentration comparison experiment.

Table S5. Photoluminescence lifetime for TADF monomers and TADF P-dots.

Samples	R ²	A ₁	A ₂	τ_1 (ns)	τ_2 (ns)	τ_{ave} (ns)
1 (Air)	0.999	0.984	0.016	12	85	20
1 (Ar)	0.999	0.976	0.024	20	1068	615
P-dot (1) (Air)	0.997	0.983	0.017	18	1075	555
P-dot (1) (Ar)	0.993	0.982	0.018	24	1454	776
2 (Air)	0.999	0.945	0.055	13	323	196
2 (Ar)	0.993	0.966	0.034	20	2424	1967
P-dot (2) (Air)	0.994	1.000	0.0003	18	1104	38
P-dot (2) (Ar)	0.968	1.000	7.67E-05	15	1359	24
3 (Air)	0.998	0.978	0.022	12	271	99
3 (Ar)	0.998	0.995	0.005	19	953	207
P-dot (3) (Air)	0.984	0.992	0.008	20	260	43
P-dot (3) (Ar)	0.984	0.993	0.007	19	300	47

^a Photoluminescence lifetime determined by the origin software.

Table S6. Triplet lifetime for TADF monomers.

Samples	A_1	A_2	τ_1 (ns)	τ_2 (ns)	τ_{ave} (ns)
1 (Air)	0.423	0.577	2	53	52
1 (Ar)	0.395	0.605	2	1853	1851
2 (Air)	0.158	0.842	3	393	392
2 (Ar)	0.254	0.746	5	3186	3185
3 (Air)	0.672	0.328	13	221	198
3 (Ar)	0.911	0.089	21	1402	1222

^a Triplet lifetime determined by the origin software.

Table S7. Triplet lifetime for TADF P-dots.

Samples	A_1	A_2	A_3	τ_1 (ns)	τ_2 (ns)	τ_3 (ns)	τ_{ave} (ns)
P-dot (1) (Air)	0.529	0.194	0.277	4	100	1590	1521
P-dot (1) (Ar)	0.541	0.230	0.229	3	167	1681	1537
P-dot (2) (Air)	0.488	0.282	0.230	2	54	1349	1283
P-dot (2) (Ar)	0.525	0.235	0.240	1	3.00E-04	1112	1108
P-dot (3) (Air)	0.433	0.431	0.136	1	12	495	458
P-dot (3) (Ar)	0.684	0.220	0.096	1	21	521	469

^a Triplet lifetime determined by the origin software.

Table S8. Scintillation decay lifetime for TADF P-dots.

Samples	τ_1 (ns)	A_1	τ_2 (ns)	A_2	τ_{ave} (ns) ^a
P-dots (1)	16	98.6	1020	1.4	500
P-dots (2)	8.2	99.4	764	0.6	280
P-dots (3)	8.1	99.7	379	0.3	50

^aThe data was measured with time range of 10 μs , fitted by two component decay curve.

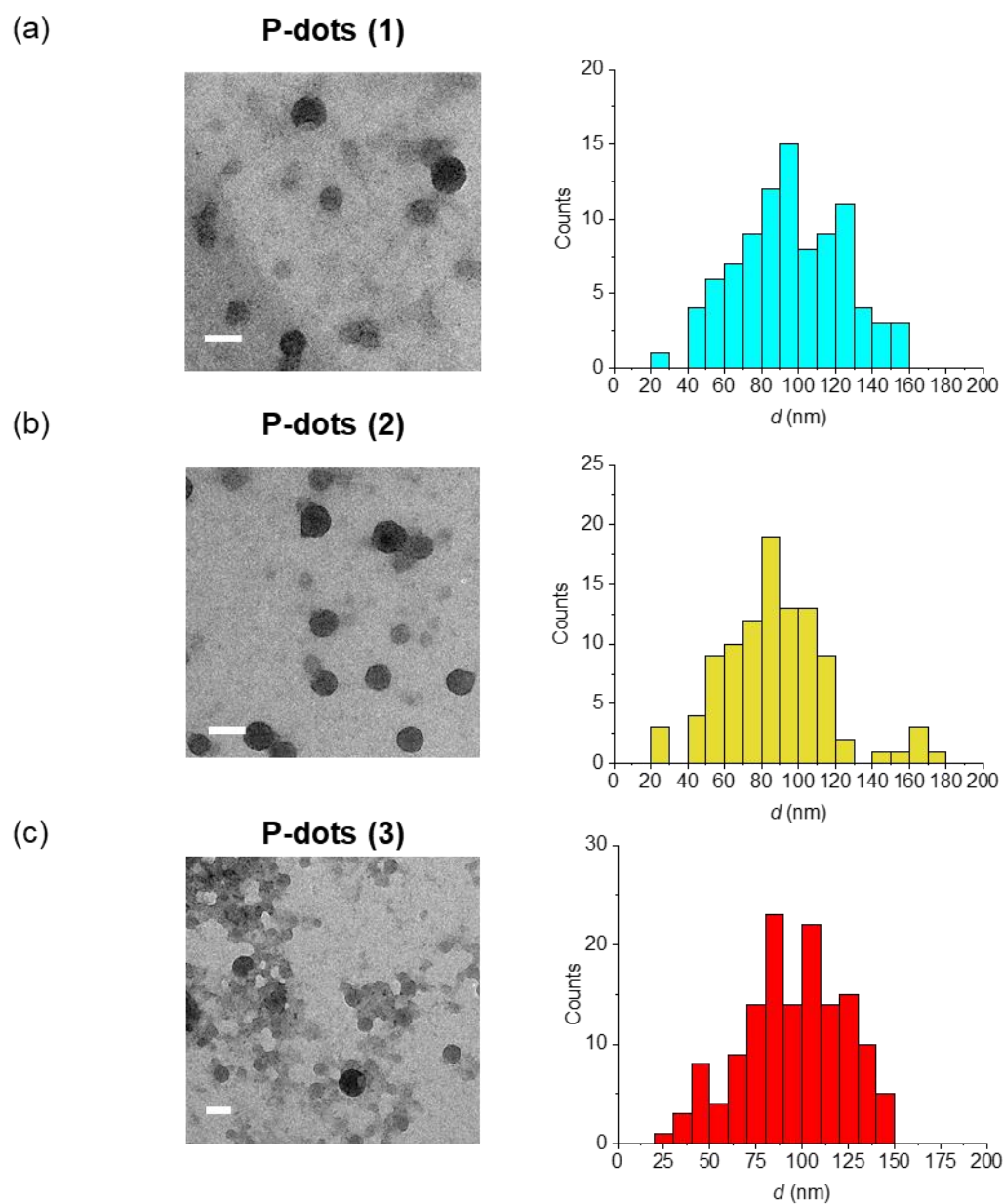


Figure S1. TEM images (left) and size distribution histogram (right) for **P-dots (1)** (a), **P-dots (2)** (b), and **P-dots 3** (c).

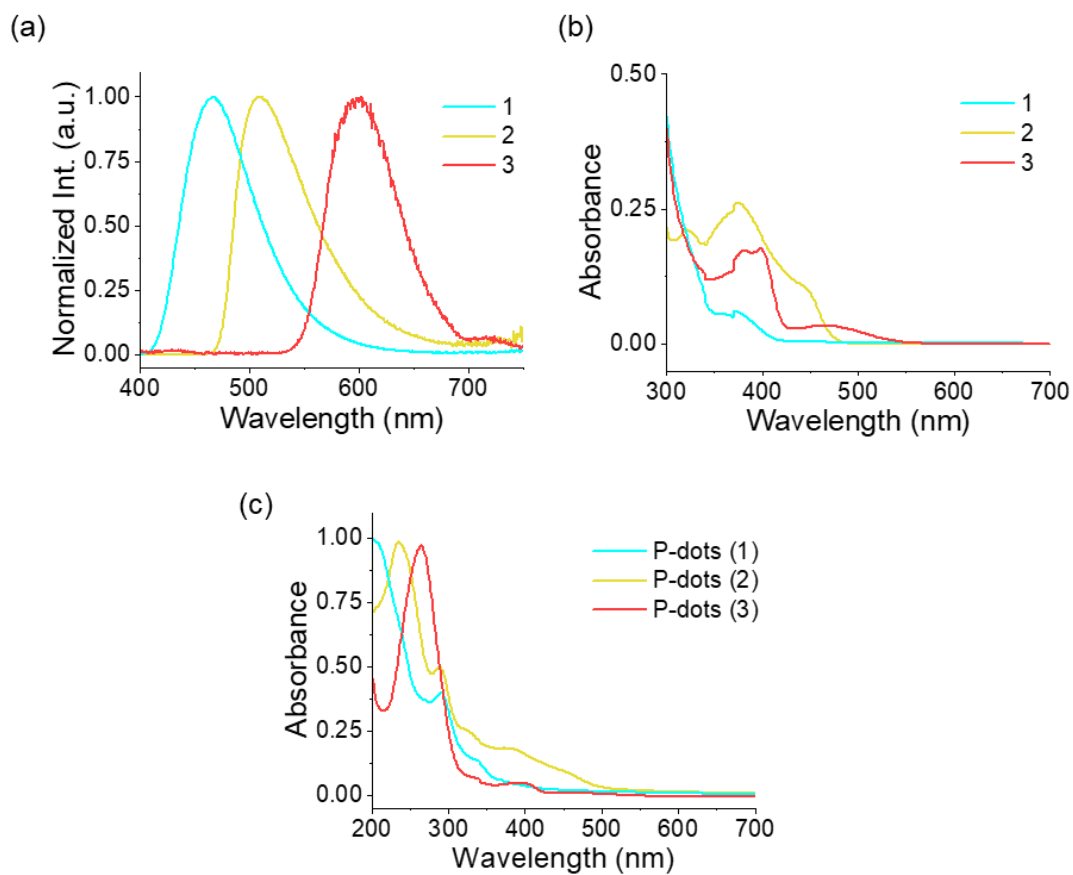


Figure S2. (a) Photoluminescence excited at 355 nm and (b) absorption spectra of TADF monomer molecules (**1** (sky blue), **2** (yellow), **3** (red)) in toluene. (c) Absorption spectra of **P-dots (1)** (sky blue), **P-dots (2)** (yellow), and **P-dots 3** (red) measured with the maximum absorption restricted to around 1 to ensure spectral clarity.

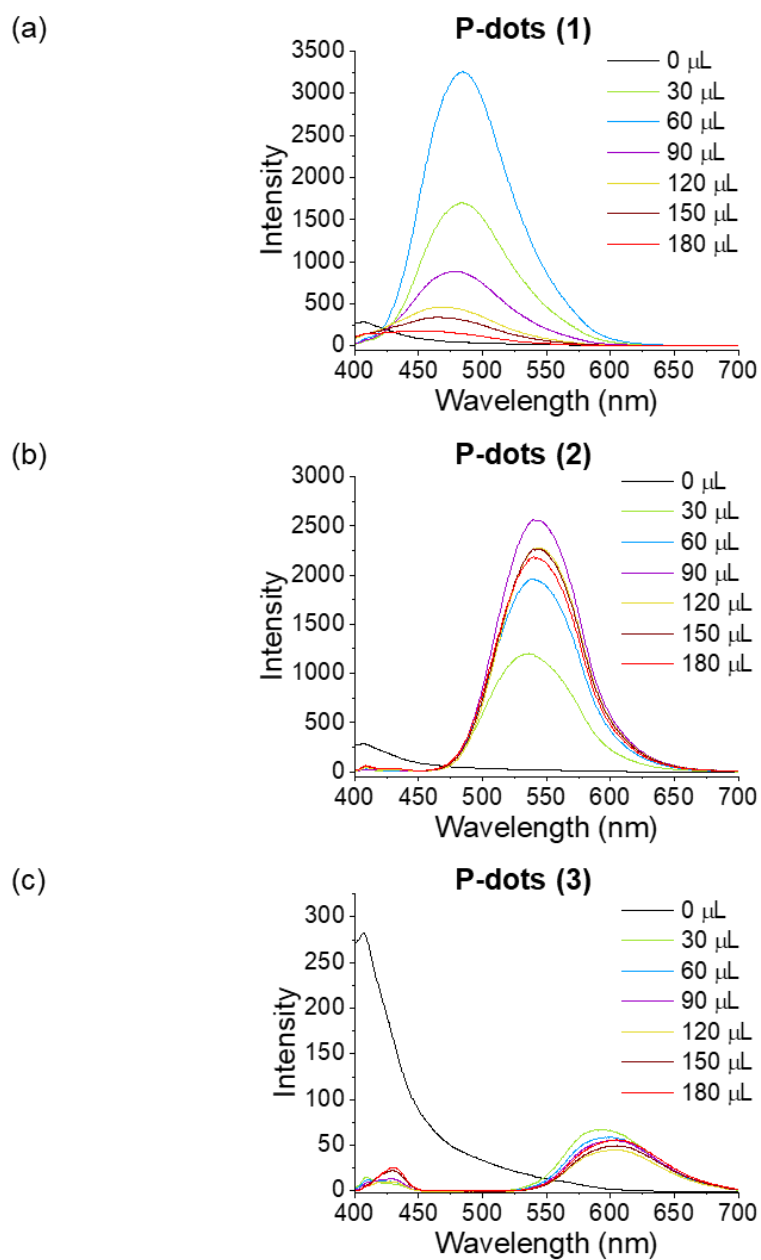


Figure S3. Photoluminescence spectra of (a) **P-dots (1)**, (b) **P-dots (2)** and (c) **P-dots (3)** excited at 355 nm. The volume of the TADF molecules' solution when synthesized is shown. The detailed amounts of each are shown in Table S1.

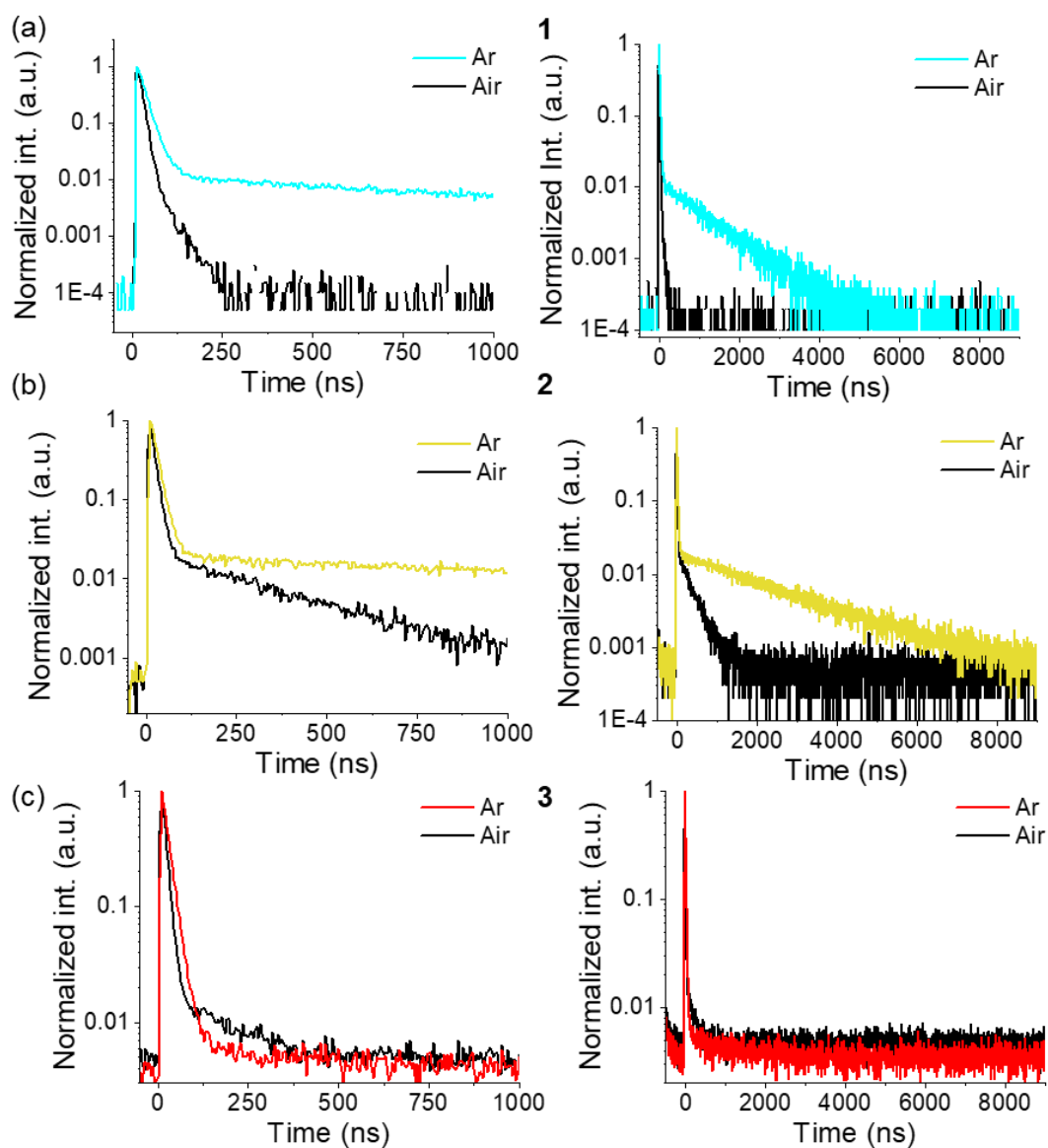


Figure S4. Time-resolved photoluminescence decay curves for **1** (a), **2** (b), and **3** (c). Measurements taken under argon atmosphere are shown in color (sky blue, yellow and red), while those taken in the presence of oxygen are shown in black. All decay curves were obtained with excitation at 365 nm. Curve fitting were performed by three-component exponential equation $y = y_0 + A_1 * \exp(-x_1 / \tau_1) + A_2 * \exp(-x_2 / \tau_2) + A_3 * \exp(-x_3 / \tau_3)$, $\tau = \Sigma A_i \tau_i^2 / \Sigma A_i \tau_i$.

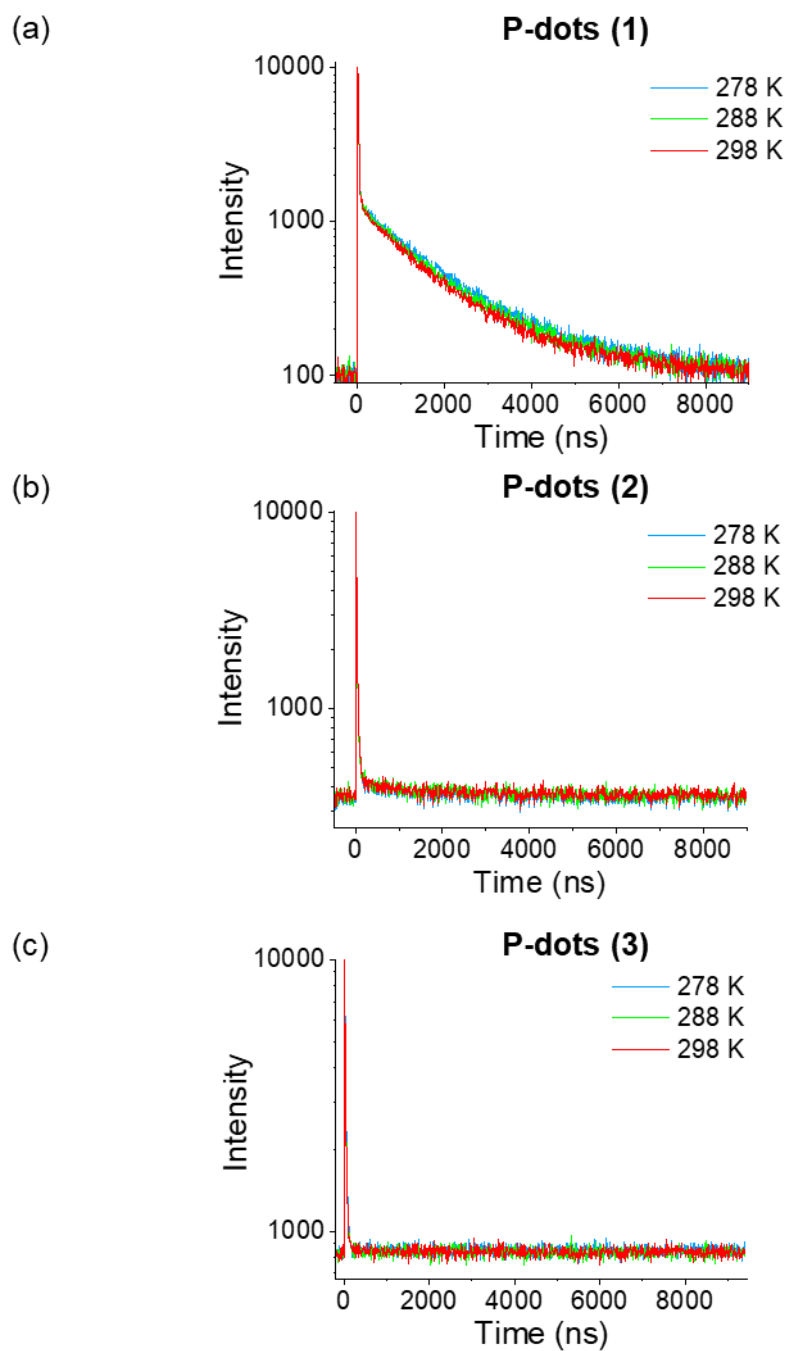


Figure S5. Temperature dependence experiments for time-resolved photoluminescence decay curves. Measurements were done under aerobic condition at the 278, 288 and 298 K.

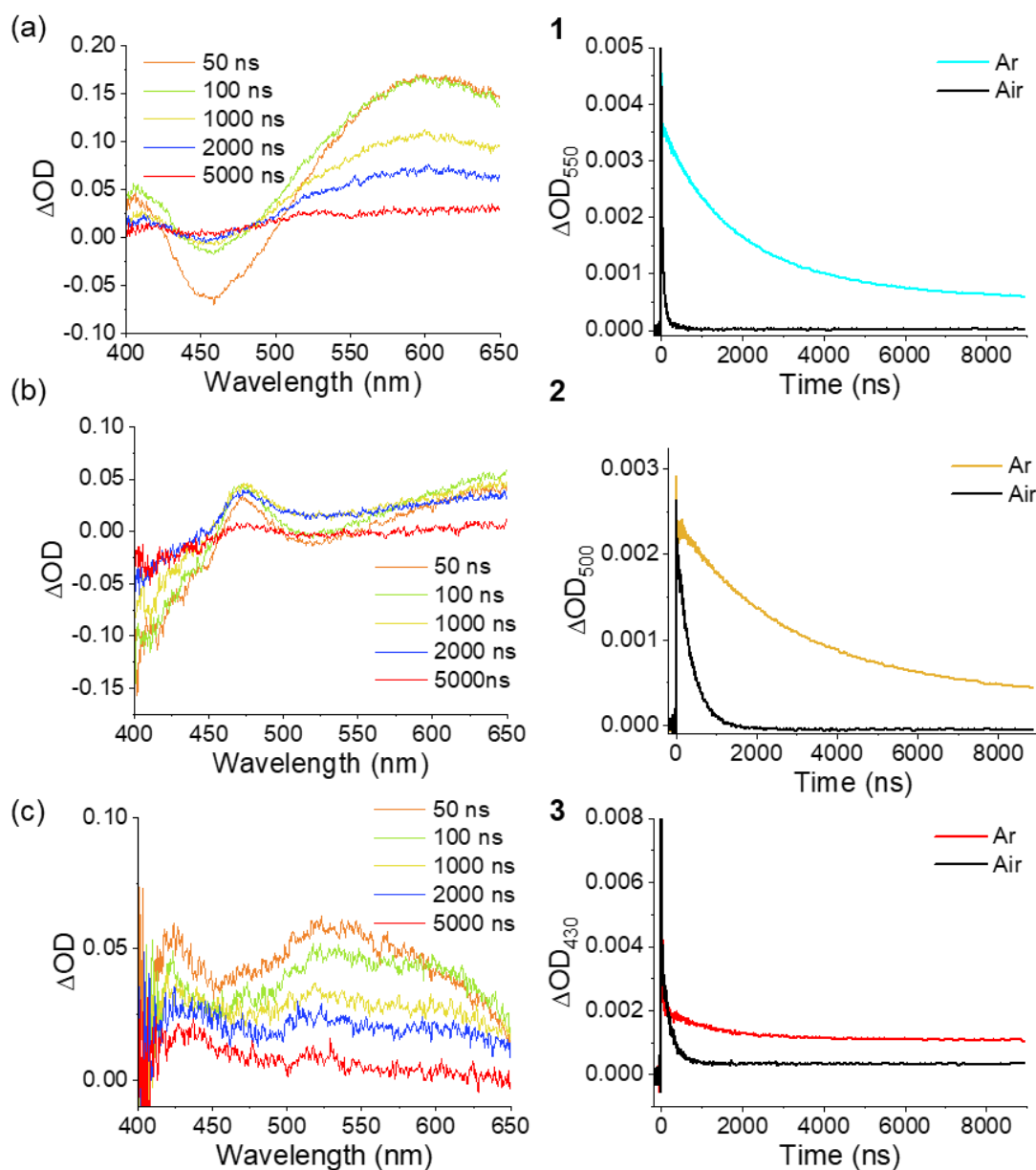


Figure S6. (Left) Transient absorption spectra and time profiles for TADF monomer molecules (**1** (a), **2** (b), **3** (c)) in toluene obtained by laser excitation, with parameters of Gate Width: 30.0 ns, and Slit / Resolution: 5 mm / 85.0 nm. **(Right)** Measurements were made using a nanosecond multi-channel system. Time profiles for TADF monomer molecules (**1** (a), **2** (b), **3** (c)) in toluene were obtained by the RIPT method (pump frequency: 1000 Hz; accumulation number \times pump: 250 \times 500.). Measurements taken under argon atmosphere are shown in colors (sky blue, yellow, and red), while those taken in the presence of oxygen are shown in black. Curve fitting were performed by three-component exponential equation $y = y_0 + A_1 * \exp(-x_1 / \tau_1) + A_2 * \exp(-x_2 / \tau_2)$, $\tau = \sum A_i \tau_i^2 / \sum A_i \tau_i$.

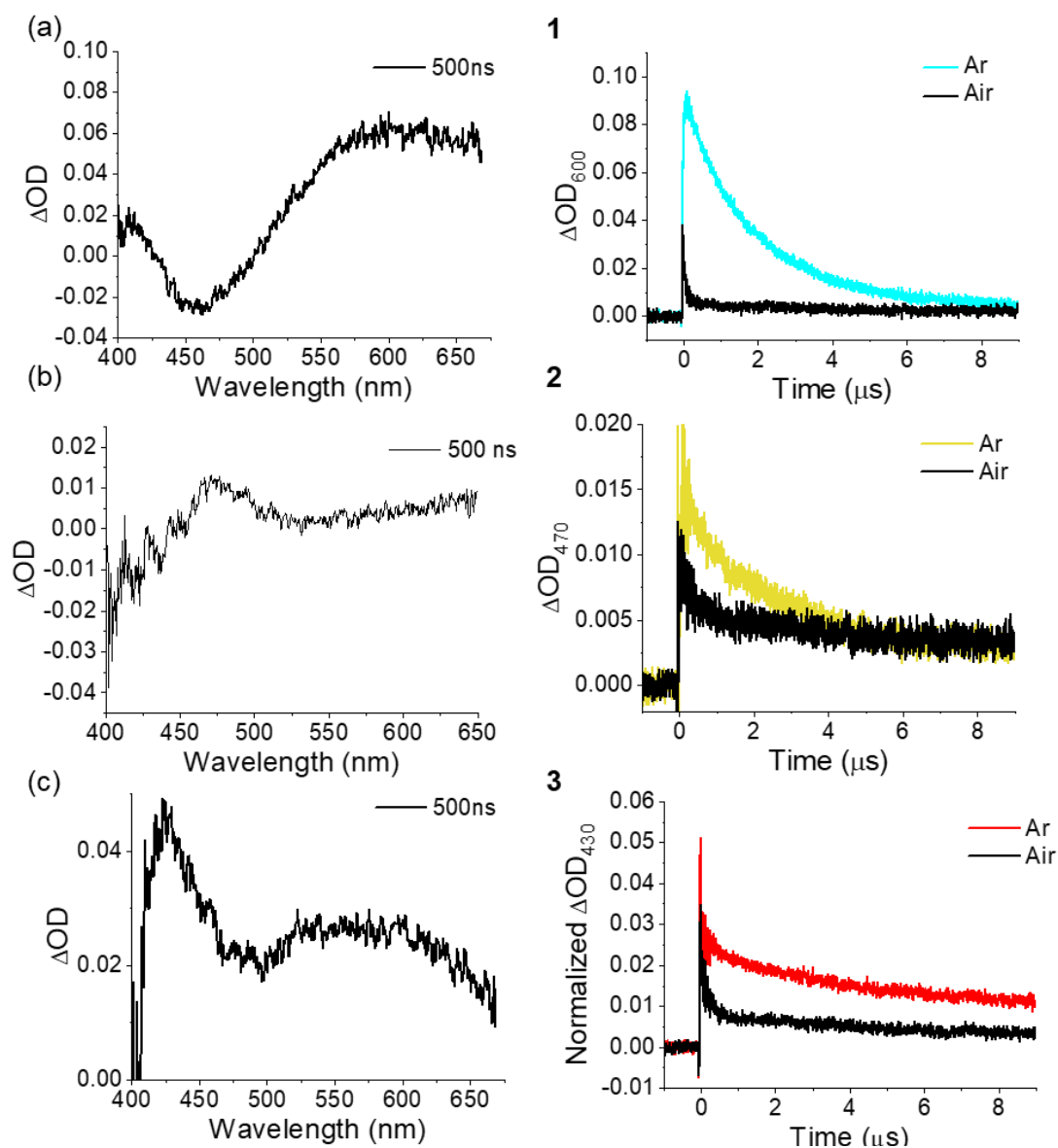


Figure S7. (Left) Transient absorption spectra obtained by pulse radiolysis for TADF monomer molecules (**1** (a), **2** (b), **3** (c)) in toluene at 500 ns after radiation using an L-band LINAC-accelerated electron pulse (28 MeV) as the excitation source. (Right) Time profiles of absorption at 600 nm (**1** (a)), 470 nm (**2** (b)), and 430 nm (**3** (c)). Measurements taken under argon atmosphere are shown in colors (sky blue, yellow and red), while those taken in the presence of oxygen are shown in black. Curve fitting performed by origin software using two-component exponential equation ($y = y_0 + A_1 * \exp(-x_1 / \tau_1) + A_2 * \exp(-x_2 / \tau_2)$, $\tau = \Sigma A_i \tau_i^2 / \Sigma A_i \tau_i$).

Supporting references.

- S1. D. Asanuma, H. T. Minh Nguyen, Z. Liu, S. Tojo, H. Shigemitsu, M. Yamaji, K. Kawai, T. Mori, T. Kida, G. Pratx, M. Fujitsuka and Y. Osakada, *Nanoscale Adv.*, 2023, **5**, 3424-3427.
- S2. T. Nakagawa, K. Okamoto, H. Hanada and R. Katoh, *Opt. Lett.*, 2016, **41**, 1498-1501.
- S3. L. M. Bollinger and G. E. Thomas, *Rev. Sci. Instrum.*, 1961, **32**, 1044-1050.